

Measurement of the Branching Fractions of Exclusive $\overline{B} \rightarrow D/D^*/D^{(*)}\pi\ell^-\bar{\nu}_\ell$ Decays in Events Tagged by a Fully Reconstructed B Meson

The *BABAR* Collaboration

October 25, 2008

Abstract

We present a measurement of the branching fractions for $\overline{B} \rightarrow D/D^*/D^{(*)}\pi\ell^-\bar{\nu}_\ell$ decays based on 341.1 fb^{-1} of data collected at the $\Upsilon(4S)$ resonance with the *BABAR* detector at the PEP-II e^+e^- storage rings. Events are tagged by fully reconstructing one of the B mesons in a hadronic decay mode. We obtain $\mathcal{B}(B^- \rightarrow D^0\ell^-\bar{\nu}_\ell) = (2.33 \pm 0.09 \text{ (stat.)} \pm 0.09 \text{ (syst.)})\%$, $\mathcal{B}(B^- \rightarrow D^{*0}\ell^-\bar{\nu}_\ell) = (5.83 \pm 0.15 \text{ (stat.)} \pm 0.30 \text{ (syst.)})\%$, $\mathcal{B}(\overline{B}^0 \rightarrow D^+\ell^-\bar{\nu}_\ell) = (2.21 \pm 0.11 \text{ (stat.)} \pm 0.12 \text{ (syst.)})\%$, $\mathcal{B}(\overline{B}^0 \rightarrow D^{*+}\ell^-\bar{\nu}_\ell) = (5.49 \pm 0.16 \text{ (stat.)} \pm 0.25 \text{ (syst.)})\%$, $\mathcal{B}(B^- \rightarrow D^+\pi^-\ell^-\bar{\nu}_\ell) = (0.42 \pm 0.06 \text{ (stat.)} \pm 0.03 \text{ (syst.)})\%$, $\mathcal{B}(B^- \rightarrow D^{*+}\pi^-\ell^-\bar{\nu}_\ell) = (0.59 \pm 0.05 \text{ (stat.)} \pm 0.04 \text{ (syst.)})\%$, $\mathcal{B}(\overline{B}^0 \rightarrow D^0\pi^+\ell^-\bar{\nu}_\ell) = (0.43 \pm 0.08 \text{ (stat.)} \pm 0.03 \text{ (syst.)})\%$ and $\mathcal{B}(\overline{B}^0 \rightarrow D^{*0}\pi^+\ell^-\bar{\nu}_\ell) = (0.48 \pm 0.08 \text{ (stat.)} \pm 0.04 \text{ (syst.)})\%$.

Contributed to the XXIIIrd International Symposium on Lepton and Photon Interactions at High Energies, 8/13 – 8/18/2007, Daegu, Korea

Stanford Linear Accelerator Center, Stanford University, Stanford, CA 94309

Work supported in part by Department of Energy contract DE-AC03-76SF00515.

The BABAR Collaboration,

B. Aubert, M. Bona, D. Boutigny, Y. Karyotakis, J. P. Lees, V. Poireau, X. Prudent, V. Tisserand,
A. Zghiche

*Laboratoire de Physique des Particules, IN2P3/CNRS et Université de Savoie, F-74941 Annecy-Le-Vieux,
France*

J. Garra Tico, E. Grauges

Universitat de Barcelona, Facultat de Física, Departament ECM, E-08028 Barcelona, Spain

L. Lopez, A. Palano, M. Pappagallo

Università di Bari, Dipartimento di Fisica and INFN, I-70126 Bari, Italy

G. Eigen, B. Stugu, L. Sun

University of Bergen, Institute of Physics, N-5007 Bergen, Norway

G. S. Abrams, M. Battaglia, D. N. Brown, J. Button-Shafer, R. N. Cahn, Y. Groysman, R. G. Jacobsen,
J. A. Kadyk, L. T. Kerth, Yu. G. Kolomensky, G. Kukartsev, D. Lopes Pegna, G. Lynch, L. M. Mir,
T. J. Orimoto, I. L. Osipenkov, M. T. Ronan,¹ K. Tackmann, T. Tanabe, W. A. Wenzel

Lawrence Berkeley National Laboratory and University of California, Berkeley, California 94720, USA

P. del Amo Sanchez, C. M. Hawkes, A. T. Watson

University of Birmingham, Birmingham, B15 2TT, United Kingdom

H. Koch, T. Schroeder

Ruhr Universität Bochum, Institut für Experimentalphysik 1, D-44780 Bochum, Germany

D. Walker

University of Bristol, Bristol BS8 1TL, United Kingdom

D. J. Asgeirsson, T. Cuhadar-Donszelmann, B. G. Fulsom, C. Hearty, T. S. Mattison, J. A. McKenna

University of British Columbia, Vancouver, British Columbia, Canada V6T 1Z1

A. Khan, M. Saleem, L. Teodorescu

Brunel University, Uxbridge, Middlesex UB8 3PH, United Kingdom

V. E. Blinov, A. D. Bukin, V. P. Druzhinin, V. B. Golubev, A. P. Onuchin, S. I. Serednyakov,
Yu. I. Skovpen, E. P. Solodov, K. Yu. Todyshev

Budker Institute of Nuclear Physics, Novosibirsk 630090, Russia

M. Bondioli, S. Curry, I. Eschrich, D. Kirkby, A. J. Lankford, P. Lund, M. Mandelkern, E. C. Martin,
D. P. Stoker

University of California at Irvine, Irvine, California 92697, USA

S. Abachi, C. Buchanan

University of California at Los Angeles, Los Angeles, California 90024, USA

S. D. Foulkes, J. W. Gary, F. Liu, O. Long, B. C. Shen,¹ G. M. Vitug, L. Zhang

University of California at Riverside, Riverside, California 92521, USA

¹Deceased

H. P. Paar, S. Rahatlou, V. Sharma

University of California at San Diego, La Jolla, California 92093, USA

J. W. Berryhill, C. Campagnari, A. Cunha, B. Dahmes, T. M. Hong, D. Kovalskyi, J. D. Richman

University of California at Santa Barbara, Santa Barbara, California 93106, USA

T. W. Beck, A. M. Eisner, C. J. Flacco, C. A. Heusch, J. Kroseberg, W. S. Lockman, T. Schalk,
B. A. Schumm, A. Seiden, M. G. Wilson, L. O. Winstrom

University of California at Santa Cruz, Institute for Particle Physics, Santa Cruz, California 95064, USA

E. Chen, C. H. Cheng, F. Fang, D. G. Hitlin, I. Narsky, T. Piatenko, F. C. Porter

California Institute of Technology, Pasadena, California 91125, USA

R. Andreassen, G. Mancinelli, B. T. Meadows, K. Mishra, M. D. Sokoloff

University of Cincinnati, Cincinnati, Ohio 45221, USA

F. Blanc, P. C. Bloom, S. Chen, W. T. Ford, J. F. Hirschauer, A. Kreisel, M. Nagel, U. Nauenberg,
A. Olivas, J. G. Smith, K. A. Ulmer, S. R. Wagner, J. Zhang

University of Colorado, Boulder, Colorado 80309, USA

A. M. Gabareen, A. Soffer,² W. H. Toki, R. J. Wilson, F. Winklmeier

Colorado State University, Fort Collins, Colorado 80523, USA

D. D. Altenburg, E. Feltresi, A. Hauke, H. Jasper, J. Merkel, A. Petzold, B. Spaan, K. Wacker

Universität Dortmund, Institut für Physik, D-44221 Dortmund, Germany

V. Klose, M. J. Kobel, H. M. Lacker, W. F. Mader, R. Nogowski, J. Schubert, K. R. Schubert, R. Schwierz,
J. E. Sundermann, A. Volk

Technische Universität Dresden, Institut für Kern- und Teilchenphysik, D-01062 Dresden, Germany

D. Bernard, G. R. Bonneaud, E. Latour, V. Lombardo, Ch. Thiebaux, M. Verderi

Laboratoire Leprince-Ringuet, CNRS/IN2P3, Ecole Polytechnique, F-91128 Palaiseau, France

P. J. Clark, W. Gradl, F. Muheim, S. Playfer, A. I. Robertson, J. E. Watson, Y. Xie

University of Edinburgh, Edinburgh EH9 3JZ, United Kingdom

M. Andreotti, D. Bettoni, C. Bozzi, R. Calabrese, A. Cecchi, G. Cibinetto, P. Franchini, E. Luppi,
M. Negrini, A. Petrella, L. Piemontese, E. Prencipe, V. Santoro

Università di Ferrara, Dipartimento di Fisica and INFN, I-44100 Ferrara, Italy

F. Anulli, R. Baldini-Ferrolì, A. Calcaterra, R. de Sangro, G. Finocchiaro, S. Pacetti, P. Patteri,
I. M. Peruzzi,³ M. Piccolo, M. Rama, A. Zallo

Laboratori Nazionali di Frascati dell'INFN, I-00044 Frascati, Italy

A. Buzzo, R. Contri, M. Lo Vetere, M. M. Macri, M. R. Monge, S. Passaggio, C. Patrignani, E. Robutti,
A. Santroni, S. Tosi

Università di Genova, Dipartimento di Fisica and INFN, I-16146 Genova, Italy

²Now at Tel Aviv University, Tel Aviv, 69978, Israel

³Also with Università di Perugia, Dipartimento di Fisica, Perugia, Italy

K. S. Chaisanguanthum, M. Morii, J. Wu
Harvard University, Cambridge, Massachusetts 02138, USA

R. S. Dubitzky, J. Marks, S. Schenk, U. Uwer
Universität Heidelberg, Physikalisches Institut, Philosophenweg 12, D-69120 Heidelberg, Germany

D. J. Bard, P. D. Dauncey, R. L. Flack, J. A. Nash, W. Panduro Vazquez, M. Tibbetts
Imperial College London, London, SW7 2AZ, United Kingdom

P. K. Behera, X. Chai, M. J. Charles, U. Mallik
University of Iowa, Iowa City, Iowa 52242, USA

J. Cochran, H. B. Crawley, L. Dong, V. Eyges, W. T. Meyer, S. Prell, E. I. Rosenberg, A. E. Rubin
Iowa State University, Ames, Iowa 50011-3160, USA

Y. Y. Gao, A. V. Gritsan, Z. J. Guo, C. K. Lae
Johns Hopkins University, Baltimore, Maryland 21218, USA

A. G. Denig, M. Fritsch, G. Schott
Universität Karlsruhe, Institut für Experimentelle Kernphysik, D-76021 Karlsruhe, Germany

N. Arnaud, J. Béquilleux, A. D’Orazio, M. Davier, G. Grosdidier, A. Höcker, V. Lepeltier, F. Le Diberder,
A. M. Lutz, S. Pruvot, S. Rodier, P. Roudeau, M. H. Schune, J. Serrano, V. Sordini, A. Stocchi, L. Wang,
W. F. Wang, G. Wormser

*Laboratoire de l’Accélérateur Linéaire, IN2P3/CNRS et Université Paris-Sud 11, Centre Scientifique
d’Orsay, B. P. 34, F-91898 ORSAY Cedex, France*

D. J. Lange, D. M. Wright
Lawrence Livermore National Laboratory, Livermore, California 94550, USA

I. Bingham, J. P. Burke, C. A. Chavez, J. R. Fry, E. Gabathuler, R. Gamet, D. E. Hutchcroft, D. J. Payne,
K. C. Schofield, C. Touramanis

University of Liverpool, Liverpool L69 7ZE, United Kingdom

A. J. Bevan, K. A. George, F. Di Lodovico, R. Sacco, M. Sigamani
Queen Mary, University of London, E1 4NS, United Kingdom

G. Cowan, H. U. Flaecher, D. A. Hopkins, S. Paramesvaran, F. Salvatore, A. C. Wren
*University of London, Royal Holloway and Bedford New College, Egham, Surrey TW20 0EX, United
Kingdom*

D. N. Brown, C. L. Davis
University of Louisville, Louisville, Kentucky 40292, USA

J. Allison, N. R. Barlow, R. J. Barlow, Y. M. Chia, C. L. Edgar, G. D. Lafferty, T. J. West, J. I. Yi
University of Manchester, Manchester M13 9PL, United Kingdom

J. Anderson, C. Chen, A. Jawahery, D. A. Roberts, G. Simi, J. M. Tuggle
University of Maryland, College Park, Maryland 20742, USA

G. Blaylock, C. Dallapiccola, S. S. Hertzbach, X. Li, T. B. Moore, E. Salvati, S. Saremi
University of Massachusetts, Amherst, Massachusetts 01003, USA

R. Cowan, D. Dujmic, P. H. Fisher, K. Koenke, G. Sciolla, M. Spitznagel, F. Taylor, R. K. Yamamoto,
M. Zhao, Y. Zheng
*Massachusetts Institute of Technology, Laboratory for Nuclear Science, Cambridge, Massachusetts 02139,
USA*

S. E. Mclachlin,¹ P. M. Patel, S. H. Robertson
McGill University, Montréal, Québec, Canada H3A 2T8

A. Lazzaro, F. Palombo
Università di Milano, Dipartimento di Fisica and INFN, I-20133 Milano, Italy

J. M. Bauer, L. Cremaldi, V. Eschenburg, R. Godang, R. Kroeger, D. A. Sanders, D. J. Summers,
H. W. Zhao
University of Mississippi, University, Mississippi 38677, USA

S. Brunet, D. Côté, M. Simard, P. Taras, F. B. Viaud
Université de Montréal, Physique des Particules, Montréal, Québec, Canada H3C 3J7

H. Nicholson
Mount Holyoke College, South Hadley, Massachusetts 01075, USA

G. De Nardo, F. Fabozzi,⁴ L. Lista, D. Monorchio, C. Sciacca
Università di Napoli Federico II, Dipartimento di Scienze Fisiche and INFN, I-80126, Napoli, Italy

M. A. Baak, G. Raven, H. L. Snoek
*NIKHEF, National Institute for Nuclear Physics and High Energy Physics, NL-1009 DB Amsterdam, The
Netherlands*

C. P. Jessop, K. J. Knoepfel, J. M. LoSecco
University of Notre Dame, Notre Dame, Indiana 46556, USA

G. Benelli, L. A. Corwin, K. Honscheid, H. Kagan, R. Kass, J. P. Morris, A. M. Rahimi,
J. J. Regensburger, S. J. Sekula, Q. K. Wong
Ohio State University, Columbus, Ohio 43210, USA

N. L. Blount, J. Brau, R. Frey, O. Igonkina, J. A. Kolb, M. Lu, R. Rahmat, N. B. Sinev, D. Strom,
J. Strube, E. Torrence
University of Oregon, Eugene, Oregon 97403, USA

N. Gagliardi, A. Gaz, M. Margoni, M. Morandin, A. Pompili, M. Posocco, M. Rotondo, F. Simonetto,
R. Stroili, C. Voci
Università di Padova, Dipartimento di Fisica and INFN, I-35131 Padova, Italy

E. Ben-Haim, H. Briand, G. Calderini, J. Chauveau, P. David, L. Del Buono, Ch. de la Vaissière,
O. Hamon, Ph. Leruste, J. Malcès, J. Ocariz, A. Perez, J. Prendki
*Laboratoire de Physique Nucléaire et de Hautes Energies, IN2P3/CNRS, Université Pierre et Marie
Curie-Paris6, Université Denis Diderot-Paris7, F-75252 Paris, France*

⁴Also with Università della Basilicata, Potenza, Italy

L. Gladney

University of Pennsylvania, Philadelphia, Pennsylvania 19104, USA

M. Biasini, R. Covarelli, E. Manoni

Università di Perugia, Dipartimento di Fisica and INFN, I-06100 Perugia, Italy

C. Angelini, G. Batignani, S. Bettarini, M. Carpinelli,⁵ R. Cenci, A. Cervelli, F. Forti, M. A. Giorgi,
A. Lusiani, G. Marchiori, M. A. Mazur, M. Morganti, N. Neri, E. Paoloni, G. Rizzo, J. J. Walsh

Università di Pisa, Dipartimento di Fisica, Scuola Normale Superiore and INFN, I-56127 Pisa, Italy

J. Biesiada, P. Elmer, Y. P. Lau, C. Lu, J. Olsen, A. J. S. Smith, A. V. Telnov

Princeton University, Princeton, New Jersey 08544, USA

E. Baracchini, F. Bellini, G. Cavoto, D. del Re, E. Di Marco, R. Faccini, F. Ferrarotto, F. Ferroni,
M. Gaspero, P. D. Jackson, L. Li Gioi, M. A. Mazzoni, S. Morganti, G. Piredda, F. Polci, F. Renga,
C. Voena

Università di Roma La Sapienza, Dipartimento di Fisica and INFN, I-00185 Roma, Italy

M. Ebert, T. Hartmann, H. Schröder, R. Waldi

Universität Rostock, D-18051 Rostock, Germany

T. Adye, G. Castelli, B. Franek, E. O. Olaiya, W. Roethel, F. F. Wilson

Rutherford Appleton Laboratory, Chilton, Didcot, Oxon, OX11 0QX, United Kingdom

S. Emery, M. Escalier, A. Gaidot, S. F. Ganzhur, G. Hamel de Monchenault, W. Kozanecki, G. Vasseur,
Ch. Yèche, M. Zito

DSM/Daphnia, CEA/Saclay, F-91191 Gif-sur-Yvette, France

X. R. Chen, H. Liu, W. Park, M. V. Purohit, R. M. White, J. R. Wilson,

University of South Carolina, Columbia, South Carolina 29208, USA

M. T. Allen, D. Aston, R. Bartoldus, P. Bechtle, R. Claus, J. P. Coleman, M. R. Convery, J. C. Dingfelder,
J. Dorfan, G. P. Dubois-Felsmann, W. Dunwoodie, R. C. Field, T. Glanzman, S. J. Gowdy, M. T. Graham,
P. Grenier, C. Hast, W. R. Innes, J. Kaminski, M. H. Kelsey, H. Kim, P. Kim, M. L. Kocian,
D. W. G. S. Leith, S. Li, S. Luitz, V. Luth, H. L. Lynch, D. B. MacFarlane, H. Marsiske, R. Messner,
D. R. Muller, S. Nelson, C. P. O'Grady, I. Ofte, A. Perazzo, M. Perl, T. Pulliam, B. N. Ratcliff,
A. Roodman, A. A. Salnikov, R. H. Schindler, J. Schwiening, A. Snyder, D. Su, S. Sun, M. K. Sullivan,
K. Suzuki, S. K. Swain, J. M. Thompson, J. Va'vra, A. P. Wagner, M. Weaver, W. J. Wisniewski,
M. Wittgen, D. H. Wright, A. K. Yarritu, K. Yi, C. C. Young, V. Ziegler

Stanford Linear Accelerator Center, Stanford, California 94309, USA

P. R. Burchat, A. J. Edwards, S. A. Majewski, T. S. Miyashita, B. A. Petersen, L. Wilden

Stanford University, Stanford, California 94305-4060, USA

S. Ahmed, M. S. Alam, R. Bula, J. A. Ernst, V. Jain, B. Pan, M. A. Saeed, F. R. Wappler, S. B. Zain

State University of New York, Albany, New York 12222, USA

M. Krishnamurthy, S. M. Spanier, B. J. Wogsland

University of Tennessee, Knoxville, Tennessee 37996, USA

⁵Also with Università di Sassari, Sassari, Italy

R. Eckmann, J. L. Ritchie, A. M. Ruland, C. J. Schilling, R. F. Schwitters
University of Texas at Austin, Austin, Texas 78712, USA

J. M. Izen, X. C. Lou, S. Ye
University of Texas at Dallas, Richardson, Texas 75083, USA

F. Bianchi, F. Gallo, D. Gamba, M. Pelliccioni
Università di Torino, Dipartimento di Fisica Sperimentale and INFN, I-10125 Torino, Italy

M. Bomben, L. Bosisio, C. Cartaro, F. Cossutti, G. Della Ricca, L. Lanceri, L. Vitale
Università di Trieste, Dipartimento di Fisica and INFN, I-34127 Trieste, Italy

V. Azzolini, N. Lopez-March, F. Martinez-Vidal,⁶ D. A. Milanes, A. Oyanguren
IFIC, Universitat de Valencia-CSIC, E-46071 Valencia, Spain

J. Albert, Sw. Banerjee, B. Bhuyan, K. Hamano, R. Kowalewski, I. M. Nugent, J. M. Roney, R. J. Sobie
University of Victoria, Victoria, British Columbia, Canada V8W 3P6

P. F. Harrison, J. Ilic, T. E. Latham, G. B. Mohanty
Department of Physics, University of Warwick, Coventry CV4 7AL, United Kingdom

H. R. Band, X. Chen, S. Dasu, K. T. Flood, J. J. Hollar, P. E. Kutter, Y. Pan, M. Pierini, R. Prepost,
S. L. Wu
University of Wisconsin, Madison, Wisconsin 53706, USA

H. Neal
Yale University, New Haven, Connecticut 06511, USA

⁶Also with Universitat de Barcelona, Facultat de Fisica, Departament ECM, E-08028 Barcelona, Spain

1 Introduction

The determination of the individual exclusive branching fractions of $\overline{B} \rightarrow X_c \ell^- \bar{\nu}_\ell$ decays⁷ is important for the study of the dynamics of semileptonic decays of the B meson. Improvement in the knowledge of these branching fractions is also desired to reduce the systematic uncertainty in the measurements of the Cabibbo-Kobayashi-Maskawa [1] elements $|V_{cb}|$ and $|V_{ub}|$. This is exemplified by the fact that one of the leading sources of systematic uncertainty in the extraction of $|V_{cb}|$ from the exclusive decay $\overline{B} \rightarrow D^* \ell^- \bar{\nu}_\ell$ is our limited knowledge of the background due to $\overline{B} \rightarrow D^* \pi \ell^- \bar{\nu}_\ell$ [2]. Improvements in our knowledge of $\overline{B} \rightarrow X_c \ell^- \bar{\nu}_\ell$ decays will also benefit the accuracy of the extraction of $|V_{ub}|$, as analyses are extending into kinematical regions where these decays represent a sizable background.

Measurements of the largest B meson branching fraction, $\mathcal{B}(\overline{B}^0 \rightarrow D^{*+} \ell^- \bar{\nu}_\ell)$, by the CLEO, LEP, *BABAR*, and BELLE experiments, based on different reconstruction techniques, show sizable differences, resulting in an average value [3] with a probability of only 5%, thus indicating uncertainties that may be larger than stated and/or sizable correlations among the different measurements. The world average for the charged mode, $\mathcal{B}(B^- \rightarrow D^{*0} \ell^- \bar{\nu}_\ell)$, has a larger uncertainty (about 8%) and is dominated by the CLEO result [4]. Recently *BABAR* has measured the form-factor parameters and the branching fraction of the $B^- \rightarrow D^{*0} \ell^- \bar{\nu}_\ell$ decay mode, with an accuracy comparable to the world average [5]. Few measurements are available for the exclusive decays $\overline{B} \rightarrow D \ell^- \bar{\nu}_\ell$ and the uncertainties are in general larger due to larger background levels and less stringent kinematic constraints (i.e. no narrow D^* mass peak) [2].

The first measurements of the fractions of D^{**} states in semileptonic B decays were reported by the ALEPH [6], DELPHI [7, 8], and OPAL [9] collaborations at LEP, and by CLEO [10] at CESR. We denote by D^{**} any hadronic final state containing a charm meson with total mass above that of the D^* state, thereby including both D_J excited mesons (narrow and broad states) and $D^{(*)+n\pi}$ non-resonant states, with $n \geq 1$. More recently, new results have been obtained by the D0 [11] experiment at the Tevatron.

While $\overline{B} \rightarrow D \ell^- \bar{\nu}_\ell$ and $\overline{B} \rightarrow D^* \ell^- \bar{\nu}_\ell$ decays account for about 70% of the $\overline{B} \rightarrow X \ell^- \bar{\nu}_\ell$ branching fraction, the contributions of other states, including resonant and non-resonant $D^{(*)}n\pi$ decays, are not yet well measured and are a possible explanation of the observed difference between the inclusive rate and the sum of the measured exclusive rates. BELLE has recently reported the determination of the $D^{(*)} \pi \ell \bar{\nu}_\ell$ decay branching fraction [12], and *BABAR* [13] has reported a measurement of the relative branching fractions $\Gamma(\overline{B} \rightarrow D/D^*/D^{**} \ell^- \bar{\nu}_\ell)/\Gamma(\overline{B} \rightarrow DX \ell^- \bar{\nu}_\ell)$. In this paper, we present measurements of the branching fractions for $\overline{B} \rightarrow D/D^*/D^{(*)} \pi \ell^- \bar{\nu}_\ell$ decays⁸, separately for charged and neutral B mesons. These exclusive branching fractions are normalized to a sample of inclusive $\overline{B} \rightarrow X \ell^- \bar{\nu}_\ell$ events.

2 The *BABAR* Detector and Dataset

This analysis is based on data collected with the *BABAR* detector at the PEP-II storage rings. The total integrated luminosity of the dataset is 341.1 fb⁻¹ collected on the $\Upsilon(4S)$ resonance. The corresponding number of produced $B\overline{B}$ pairs is 378 million. An additional 36 fb⁻¹ off-peak data sample taken at a center-of-mass energy 40 MeV below the $\Upsilon(4S)$ resonance is used to study background from $e^+e^- \rightarrow f\bar{f}$ ($f = u, d, s, c, \tau$) events (continuum production). The *BABAR* detector

⁷Here X_c refers to any charm hadronic state, X_u to any charmless hadronic state, and $\ell = e, \mu$.

⁸Charge-conjugate modes are implied throughout this paper, unless explicitly stated otherwise.

is described in detail elsewhere [14]. Charged-particle trajectories are measured by a 5-layer double-sided silicon vertex tracker and a 40-layer drift chamber, both operating in a 1.5-T magnetic field. Charged-particle identification is provided by the average energy loss (dE/dx) in the tracking devices and by an internally reflecting ring-imaging Cherenkov detector. Photons are detected by a CsI(Tl) electromagnetic calorimeter (EMC). Muons are identified by the instrumented magnetic-flux return. A detailed GEANT4-based Monte Carlo (MC) simulation [15] of $B\bar{B}$ and continuum events has been used to study the detector response, its acceptance, and to test the analysis techniques. The simulation models $\bar{B} \rightarrow D^*\ell^-\bar{\nu}_\ell$ decays using calculations based on Heavy Quark Effective Theory (HQET) as in [16], $\bar{B} \rightarrow D\ell^-\bar{\nu}_\ell$ and $\bar{B} \rightarrow D^{**}(\rightarrow D^{(*)}\pi)\ell^-\bar{\nu}_\ell$ decays using the ISGW2 model [17], and $\bar{B} \rightarrow D^{(*)}\pi\ell^-\bar{\nu}_\ell$ decays using the Goity-Roberts model [18].

3 Event Selection

We select semileptonic B -meson decays in events containing a fully reconstructed B meson (B_{tag}), which allows us to constrain the kinematics, to reduce the combinatorial background, and to determine the charge and flavor of the signal B .

The analysis exploits the presence of two charmed mesons in the final state: one used for the exclusive reconstruction of the B_{tag} , and the other for the reconstruction of the semileptonic B decay.

We first reconstruct the semileptonic B decay, selecting a lepton with momentum p_ℓ^* in the center-of-mass (CM) frame higher than $0.6 \text{ GeV}/c$. Electrons from photon conversion and π^0 Dalitz decay are removed using a dedicated algorithm, which performs the reconstruction of vertices between tracks of opposite charges whose invariant mass is compatible with a photon conversion or a π^0 Dalitz decay. Candidate D^0 mesons, with the correct charge-flavor correlation with the lepton, are reconstructed in the $K^-\pi^+$, $K^-\pi^+\pi^0$, $K^-\pi^+\pi^+\pi^-$, $K_S^0\pi^+\pi^-$, $K_S^0\pi^+\pi^-\pi^0$, $K_S^0\pi^0$, K^+K^- , $\pi^+\pi^-$, and $K_S^0K_S^0$ channels, and D^+ mesons in the $K^-\pi^+\pi^+$, $K^-\pi^+\pi^+\pi^0$, $K_S^0\pi^+$, $K_S^0\pi^+\pi^0$, $K^+K^-\pi^+$, $K_S^0K^+$, and $K_S^0\pi^+\pi^+\pi^-$ channels. In events with multiple $\bar{B} \rightarrow D\ell^-\bar{\nu}_\ell$ candidates, the candidate with the largest D - ℓ vertex fit probability is selected. Candidate D^{*+} mesons are reconstructed by combining a D candidate and a pion in the $D^{*+} \rightarrow D^0\pi^+$ and $D^{*+} \rightarrow D^+\pi^0$ decays. Candidate D^{*0} mesons are reconstructed by combining a D candidate and a pion or a photon in the $D^{*0} \rightarrow D^0\pi^0$ and $D^{*0} \rightarrow D^0\gamma$ decays. In events with multiple $\bar{B} \rightarrow D^*\ell^-\bar{\nu}_\ell$ candidates, we choose the candidate with the smallest χ^2 based on the deviations from the nominal values of the D invariant mass and the invariant mass difference between the D^* and the D , using the measured uncertainty in the mass measurements.

We reconstruct B_{tag} decays of the type $\bar{B} \rightarrow DY$, where Y represents a collection of hadrons with a total charge of ± 1 , composed of $n_1\pi^\pm + n_2K^\pm + n_3K_S^0 + n_4\pi^0$, where $n_1 + n_2 \leq 5$, $n_3 \leq 2$, and $n_4 \leq 2$. Using $D^0(D^+)$ and $D^{*0}(D^{*+})$ as seeds for $B^-(\bar{B}^0)$ decays, we reconstruct about 1000 types of decay chains.

The kinematic consistency of a B_{tag} candidate with a B -meson decay is checked using two variables: the beam-energy substituted mass $m_{ES} = \sqrt{s/4 - \vec{p}_B^2}$, and the energy difference $\Delta E = E_B - \sqrt{s}/2$. Here \sqrt{s} refers to the total CM energy, and \vec{p}_B and E_B denote the momentum and energy of the B_{tag} candidate in the CM frame. For correctly identified B_{tag} decays, the m_{ES} distribution peaks at the B meson mass, while ΔE is consistent with zero. We select a B_{tag} candidate in the signal region defined as $5.27 \text{ GeV}/c^2 < m_{ES} < 5.29 \text{ GeV}/c^2$, excluding B_{tag} candidates with daughter particles in common with the charm meson or the lepton from

Table 1: Invariant mass ranges for D^{*0} and D^{*+} selection.

Mode	Selection Criteria
$D^{*0} \rightarrow D^0\pi^0$	$0.139 < M(D^{*0}) - M(D^0) < 0.145 \text{ GeV}/c^2$
$D^{*0} \rightarrow D^0\gamma$	$0.133 < M(D^{*0}) - M(D^0) < 0.151 \text{ GeV}/c^2$
$D^{*+} \rightarrow D^0\pi^+$	$0.141 < M(D^{*+}) - M(D^0) < 0.149 \text{ GeV}/c^2$
$D^{*+} \rightarrow D^+\pi^0$	$0.138 < M(D^{*+}) - M(D^+) < 0.143 \text{ GeV}/c^2$

the semileptonic B decay. In the case of multiple B_{tag} candidates, we select the one with the smallest $|\Delta E|$ value. The B_{tag} and the $D^{(*)}\ell$ candidates are required to have the correct charge-flavor correlation. Mixing effects in the $\overline{B^0}$ sample are accounted for as described in [19]. Cross-feed effects, i.e. $B_{tag}^-(\overline{B^0}_{tag})$ candidates erroneously reconstructed as a neutral (charged) B , are subtracted using the MC simulation.

Exclusive $\overline{B} \rightarrow DX\ell^-\bar{\nu}_\ell$ decays are identified by relatively loose selection criteria. We require the reconstructed ground-state charm meson invariant mass M_{D^0} (M_{D^+}) to be in the range from 1.850 (1.853) GeV/c^2 to 1.880 (1.883) GeV/c^2 and the cosine of the angle between the directions of the D candidate and the lepton in the CM frame to be less than zero, to reduce background from non- B semileptonic decays. We select $\overline{B} \rightarrow D^*X\ell^-\bar{\nu}_\ell$ decays by requiring the invariant mass difference between the D^* and the D to satisfy the selection criteria listed in Table 1.

We reconstruct $B^- \rightarrow D^{(*)+}\pi^-\ell^-\bar{\nu}_\ell$ and $\overline{B^0} \rightarrow D^{(*)0}\pi^+\ell^-\bar{\nu}_\ell$ decays starting from the corresponding $\overline{B} \rightarrow D^{(*)}X\ell^-\bar{\nu}_\ell$ samples and selecting events with only one additional reconstructed charged track that has not been used for the reconstruction of the B_{tag} , the signal $D^{(*)}$ or the lepton. For the $\overline{B^0} \rightarrow D^0\pi^+\ell^-\bar{\nu}_\ell$ and the $\overline{B^0} \rightarrow D^{*0}\pi^+\ell^-\bar{\nu}_\ell$ decays, we additionally require the invariant mass difference $M(D\pi) - M(D)$ to be greater than 0.18 GeV/c^2 to veto $\overline{B^0} \rightarrow D^{*+}\ell^-\bar{\nu}_\ell$ events. To reduce the combinatorial background in the $\overline{B^0} \rightarrow D^{*0}\pi^+\ell^-\bar{\nu}_\ell$ mode, we also require the total extra energy in the event, obtained by summing the energy of all the showers in the EMC that have not been assigned to the B_{tag} or the $D^{(*)}\ell^-$ candidates, to be less than 1 GeV.

The semileptonic B decays are identified by the missing mass squared, defined as:

$$m_{miss}^2 = (p(\Upsilon(4S)) - p(B_{tag}) - p(D^{(*)}(\pi)) - p(\ell))^2 \quad (1)$$

in terms of the particle four-momenta in the CM frame of the reconstructed final states. For correctly reconstructed signal events, the only missing particle is the neutrino, and the m_{miss}^2 peaks at zero. Other B semileptonic decays, where one particle is not reconstructed (feed-down) or erroneously added (feed-up) to the charm candidate, spread to higher or lower values of m_{miss}^2 . The selection of fully reconstructed events results in an m_{miss}^2 resolution of 0.04 GeV^2/c^4 , an order of magnitude lower compared to non-tagged analyses [20].

To obtain the B semileptonic signal yields, we perform a one-dimensional extended binned maximum likelihood fit to the m_{miss}^2 distributions, based on a method developed by R. Barlow and C. Beeston [21]. The fitted data samples are assumed to contain four different types of events:

- signal $\overline{B} \rightarrow D/D^*/D^{(*)}\pi\ell^-\bar{\nu}_\ell$
- feed-down or feed-up B semileptonic decays
- $B\overline{B}$ and continuum background
- fake lepton events.

For the fit to the $\overline{B} \rightarrow D^{(*)}\pi\ell^-\bar{\nu}_\ell$ m_{miss}^2 distributions, we also include a dedicated component corresponding to other $\overline{B} \rightarrow D^{**}(D^*\pi)\ell^-\bar{\nu}_\ell$ decays different from the exclusive mode being reconstructed. We use the Monte Carlo predictions for the different B semileptonic decay m_{miss}^2 distributions to obtain the Probability Density Functions (PDFs) to fit the data distributions. The $B\overline{B}$ and continuum background shape is also estimated by the MC simulation, and we use the off-peak data to provide the continuum background normalization. The shape of the continuum background predicted by the MC simulation is consistent with the one obtained from the off-peak data.

4 Measurement of Branching Fractions

The m_{miss}^2 distributions are compared with the results of the fits in Figure 1 for the $\overline{B} \rightarrow D/D^*\ell^-\bar{\nu}_\ell$ decays and Figure 2 for the $\overline{B} \rightarrow D^{(*)}\pi\ell^-\bar{\nu}_\ell$ decays. The fitted signal yields and the signal efficiencies, including the B_{tag} reconstruction, are listed in Table 2.

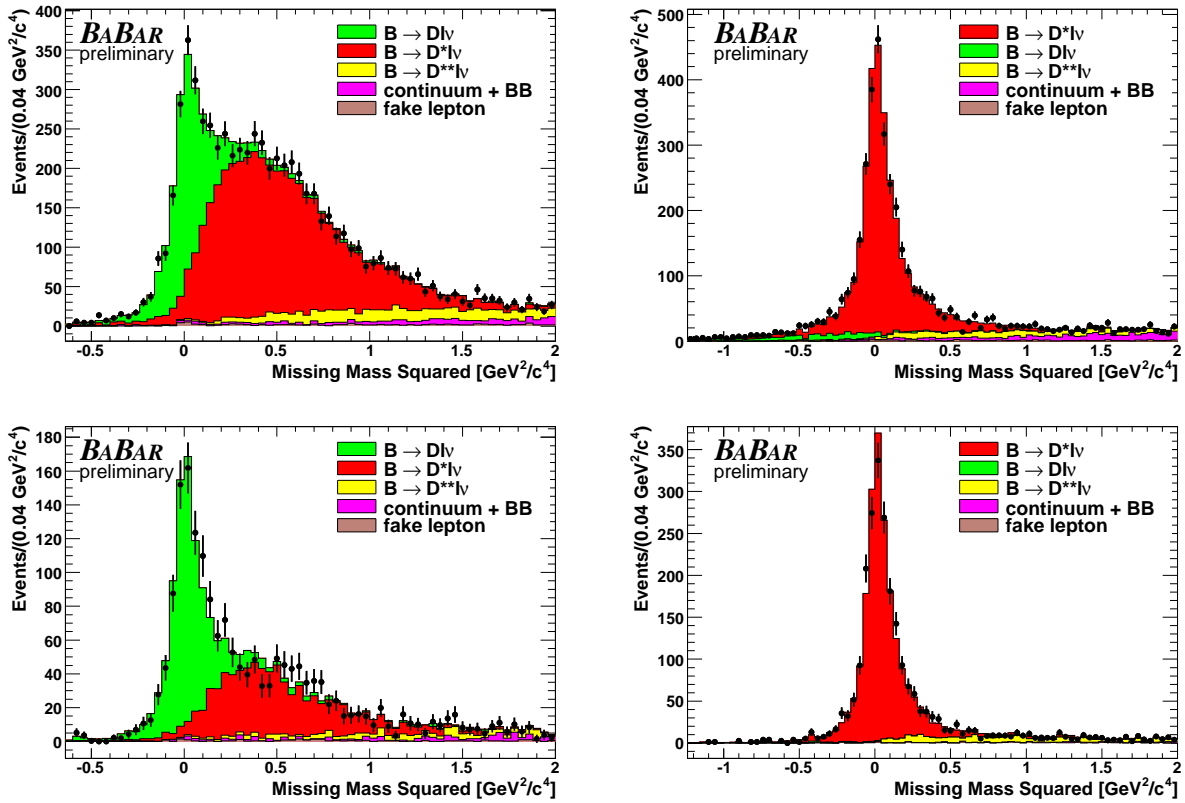


Figure 1: Fit to the m_{miss}^2 distribution for $B^- \rightarrow D^0\ell^-\bar{\nu}_\ell$ (top left), $B^- \rightarrow D^{*0}\ell^-\bar{\nu}_\ell$ (top right), $\overline{B}^0 \rightarrow D^+\ell^-\bar{\nu}_\ell$ (bottom left), and $\overline{B}^0 \rightarrow D^{*+}\ell^-\bar{\nu}_\ell$ (bottom right): the data (points with error bars) are compared to the results of the overall fit (sum of the solid histograms). The PDFs for the different fit components are stacked and shown in different colors.

In order to reduce the systematic uncertainty, the exclusive $\mathcal{B}(\overline{B} \rightarrow D^{(*)}(\pi)\ell^-\bar{\nu}_\ell)$ branching fractions are measured relative to the inclusive semileptonic branching fraction. A sample of $\overline{B} \rightarrow$

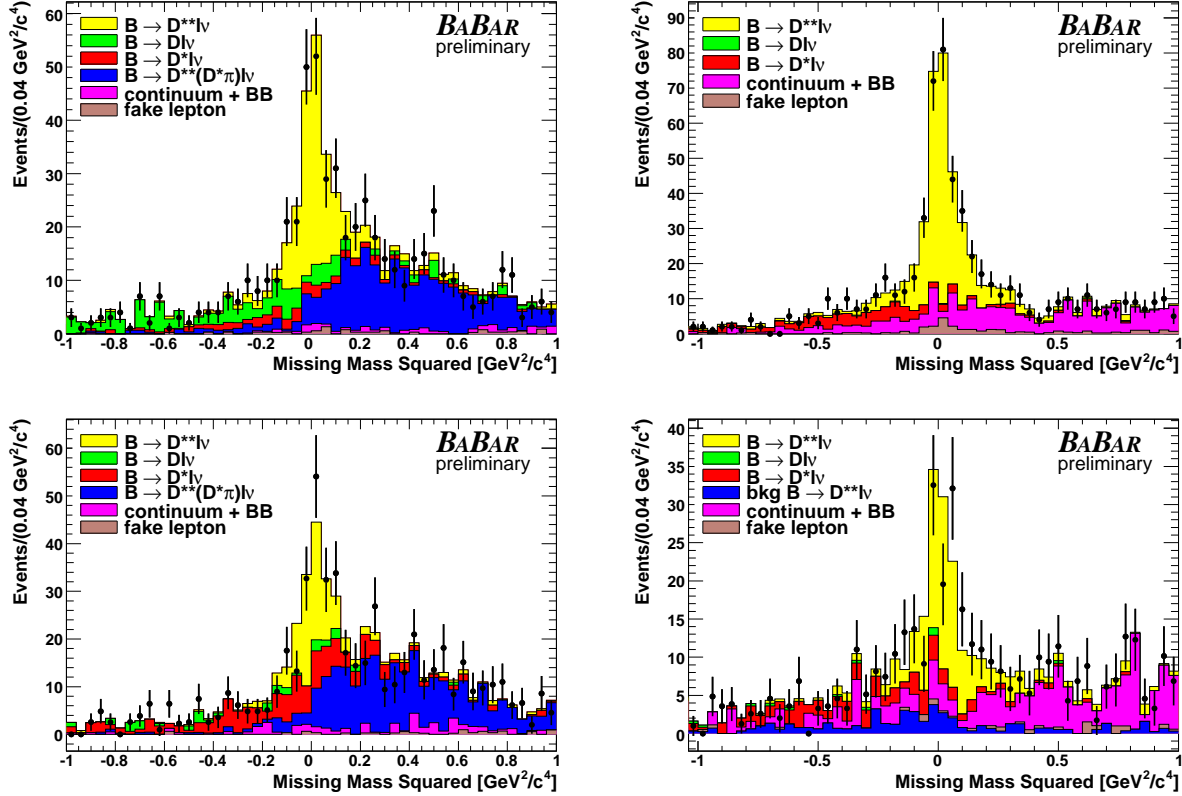


Figure 2: Fit to the m_{miss}^2 distribution for $B^- \rightarrow D^+ \pi^- \ell^- \bar{\nu}_\ell$ (top left), $B^- \rightarrow D^{*+} \pi^- \ell^- \bar{\nu}_\ell$ (top right), $\bar{B}^0 \rightarrow D^+ \ell^- \bar{\nu}_\ell$ (bottom left), and $\bar{B}^0 \rightarrow D^{*0} \pi^+ \ell^- \bar{\nu}_\ell$ (bottom right): the data (points with error bars) are compared to the results of the overall fit (sum of the solid histograms). The PDFs for the different fit components are stacked and shown in different colors.

Table 2: Signal yields and reconstruction efficiencies for the $\bar{B} \rightarrow D^{(*)}(\pi) \ell^- \bar{\nu}_\ell$ decays.

Decay Mode	N_{sig}	$\epsilon_{sig} (\times 10^{-4})$	Decay Mode	N_{sig}	$\epsilon_{sig} (\times 10^{-4})$
$B^- \rightarrow D^0 \ell^- \bar{\nu}_\ell$	1635 ± 61	1.71	$B^- \rightarrow D^+ \pi^- \ell^- \bar{\nu}_\ell$	174 ± 25	1.02
$B^- \rightarrow D^{*0} \ell^- \bar{\nu}_\ell$	3050 ± 73	1.27	$B^- \rightarrow D^{*+} \pi^- \ell^- \bar{\nu}_\ell$	306 ± 27	1.26
$\bar{B}^0 \rightarrow D^+ \ell^- \bar{\nu}_\ell$	852 ± 40	0.94	$\bar{B}^0 \rightarrow D^0 \pi^+ \ell^- \bar{\nu}_\ell$	107 ± 20	0.60
$\bar{B}^0 \rightarrow D^{*+} \ell^- \bar{\nu}_\ell$	2045 ± 55	0.91	$\bar{B}^0 \rightarrow D^{*0} \pi^+ \ell^- \bar{\nu}_\ell$	130 ± 20	0.66

$X \ell^- \bar{\nu}_\ell$ events is selected by identifying a charged lepton with CM momentum greater than 0.6 GeV/c. In the case of multiple B_{tag} candidates, we select the one reconstructed in the decay channel with the highest purity, defined as the fraction of signal events in the m_{ES} signal region. We require the lepton and the B_{tag} to have the correct charge-flavor correlation and that the lepton track has not been used to reconstruct the B_{tag} candidate. Background components peaking in the m_{ES} signal region include cascade B -meson decays (i.e. the lepton does not come directly from the B) and hadronic decays where one of the hadrons is misidentified as a lepton. These backgrounds are subtracted by using the corresponding simulated Monte Carlo distributions. The cascade- B meson decays (17.6% and 19.0% of the total m_{ES} distribution for charged and neutral

B , respectively) are reweighted to account for differences between the branching fractions used in our Monte Carlo simulation and the latest experimental measurements [22]. The total yield for the inclusive $\overline{B} \rightarrow X\ell^-\bar{\nu}_\ell$ decays is obtained from a maximum-likelihood fit to the m_{ES} distribution for the B_{tag} candidates using an ARGUS function [23] for the description of the combinatorial $B\overline{B}$ and continuum background, and a Crystal Ball function [24] for the signal. A broad peaking component is observed in the m_{ES} signal region and is included in the signal definition. This is due to real $\overline{B} \rightarrow X\ell^-\bar{\nu}_\ell$ decays for which, in the B_{tag} reconstruction, neutral particles have not been identified or have been interchanged with the semileptonic decays (e.g. a γ from radiative D^{*0} decay which belongs to the D^{*0} seed in the B_{tag} decay chain and is instead associated with a $B^- \rightarrow D^{*0}(D^0\gamma)\ell^-\bar{\nu}_\ell$ decay). This broad peaking component is modeled with additional Crystal Ball and ARGUS functions, whose parameters are fixed to the Monte Carlo prediction, except for the Crystal Ball mean value. Figure 3 shows the m_{ES} distribution for the B_{tag} candidates in the $B^- \rightarrow X\ell^-\bar{\nu}_\ell$ and $\overline{B}^0 \rightarrow X\ell^-\bar{\nu}_\ell$ sample. The fit gives 159896 ± 1361 events for the $B^- \rightarrow X\ell^-\bar{\nu}_\ell$ sample and 96771 ± 968 events for the $\overline{B}^0 \rightarrow X\ell^-\bar{\nu}_\ell$ sample.

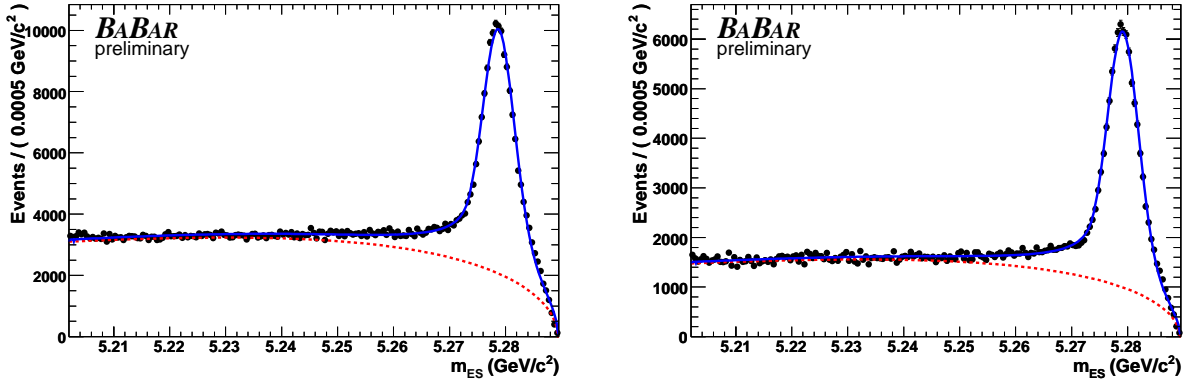


Figure 3: m_{ES} distributions for the $B^- \rightarrow X\ell^-\bar{\nu}_\ell$ (left) and $\overline{B}^0 \rightarrow X\ell^-\bar{\nu}_\ell$ (right) sample. The data (points with statistical error) are compared to the result of the fit (solid line). The dashed line shows the contribution of the combinatorial and continuum background.

The relative branching fractions $\mathcal{B}(\overline{B} \rightarrow D^{(*)}(\pi)\ell^-\bar{\nu}_\ell)/\mathcal{B}(\overline{B} \rightarrow X\ell^-\bar{\nu}_\ell)$ are obtained by correcting the signal yields obtained from the fit for the reconstruction efficiencies (estimated on $B\overline{B}$ Monte Carlo events) and using as normalization the inclusive $\overline{B} \rightarrow X\ell^-\bar{\nu}_\ell$ signal yield, following the relation

$$\frac{\mathcal{B}(\overline{B} \rightarrow D^{(*)}(\pi)\ell^-\bar{\nu}_\ell)}{\mathcal{B}(\overline{B} \rightarrow X\ell^-\bar{\nu}_\ell)} = \frac{N_{sig}}{\epsilon_{sig}} \frac{\epsilon_{sl}}{N_{sl}}.$$

Here, N_{sig} is the number of $\overline{B} \rightarrow D^{(*)}(\pi)\ell^-\bar{\nu}_\ell$ signal events for the various modes, reported in Table 2 together with the corresponding reconstruction efficiencies ϵ_{sig} . N_{sl} is the $\overline{B} \rightarrow X\ell^-\bar{\nu}_\ell$ signal yield, and ϵ_{sl} is the corresponding reconstruction efficiency, including the B_{tag} reconstruction, equal to 0.36% and 0.23%, for the $B^- \rightarrow X\ell^-\bar{\nu}_\ell$ and $\overline{B}^0 \rightarrow X\ell^-\bar{\nu}_\ell$ decays, respectively. Using the semileptonic branching fraction $\mathcal{B}(\overline{B} \rightarrow X\ell^-\bar{\nu}_\ell) = (10.78 \pm 0.18)\%$ [2] and the ratio of the B^0 and the B^+ lifetimes $\tau_{B^+}/\tau_{B^0} = 1.071 \pm 0.009$ [2], we compute the absolute branching fractions $\mathcal{B}(\overline{B} \rightarrow D^{(*)}(\pi)\ell^-\bar{\nu}_\ell)$.

5 Systematic Uncertainty

Different sources of systematic uncertainties have been estimated and are given in Tables 3 and 4. We have grouped them into several categories.

Detector-related systematics may arise from differences in the simulation of the track reconstruction and efficiency, particle identification and neutral particle reconstruction. The systematic uncertainty related to the reconstruction of charged tracks is determined by randomly removing a fraction of tracks corresponding to the uncertainty in the track finding efficiency, estimated on $e^+e^- \rightarrow \tau^+\tau^-$ data control samples. The systematic uncertainty due to the reconstruction of neutral particles in the EMC is studied by varying the resolution and efficiency to match those found in data control samples. We estimate the systematic uncertainty due to particle identification by varying the electron and muon identification efficiencies by 2% and 3%, respectively. The misidentification probabilities are varied by 15% for both electrons and muons. For the modes involving the reconstruction of D^{*+} and D^{*0} states, an additional systematic uncertainty arising from the simulation of low momentum particles is considered and is derived from the measured m_{miss}^2 distributions. From the fit to the $\overline{B} \rightarrow DX\ell^-\bar{\nu}_\ell$ m_{miss}^2 distributions in Figure 1, we extract simultaneously the signal yield of $\overline{B} \rightarrow D\ell^-\bar{\nu}_\ell$ and $\overline{B} \rightarrow D^*\ell^-\bar{\nu}_\ell$ decays. By comparing the branching fraction for the $\overline{B} \rightarrow D^*\ell^-\bar{\nu}_\ell$ decays obtained from the fit to m_{miss}^2 for $\overline{B} \rightarrow D\ell^-\bar{\nu}_\ell$ and $\overline{B} \rightarrow D^*\ell^-\bar{\nu}_\ell$ events, we evaluate the effect of the soft particle reconstruction.

We evaluate the systematic uncertainties associated with the Monte Carlo simulation of various signal and background processes. We include a systematic uncertainty of 13% (19%) on the photon conversion (π^0 Dalitz decay) reconstruction efficiency. The fraction of B cascade decays in the $\overline{B} \rightarrow X\ell^-\bar{\nu}_\ell$ sample is varied within its uncertainties and the differences in the $\overline{B} \rightarrow X\ell^-\bar{\nu}_\ell$ signal yields are included in the systematic uncertainties. Possible differences in the B_{tag} composition of the MC simulation and data can affect the efficiencies and the cross-feed between charged and neutral B events. To evaluate this effect, and to account for the limited size of the Monte Carlo sample, we assume a 30% systematic uncertainty for the cross-feed fractions and we evaluate the systematic uncertainty by looking at differences in the fitted semileptonic branching fractions as we change the cross-feed fractions. We vary the $\overline{B} \rightarrow D\ell^-\bar{\nu}_\ell$ and $\overline{B} \rightarrow D^*\ell^-\bar{\nu}_\ell$ form factors within their measured uncertainties [16] and we include a contribution due to the uncertainties on the branching fractions of the reconstructed D and D^* modes, and on the absolute branching fraction $\mathcal{B}(\overline{B} \rightarrow X\ell^-\bar{\nu}_\ell)$ used for the normalization.

We also evaluate a systematic uncertainty due to differences in the efficiency of the B_{tag} selection in the exclusive selection of $\overline{B} \rightarrow D^{(*)}(\pi)\ell^-\bar{\nu}_\ell$ decays and the inclusive $\overline{B} \rightarrow X\ell^-\bar{\nu}_\ell$ reconstruction, by using the same B_{tag} candidate selection adopted in the $\overline{B} \rightarrow X\ell^-\bar{\nu}_\ell$ reconstruction also for the $\overline{B} \rightarrow D^{(*)}(\pi)\ell^-\bar{\nu}_\ell$ decays, and taking the difference in the signal yield, corrected by the reconstruction efficiency, as a systematic uncertainty.

The uncertainty in the determination of the $\overline{B} \rightarrow X\ell^-\bar{\nu}_\ell$ yield is estimated by using an alternative fit method, which is compared to the result of the nominal m_{ES} fit to estimate the systematic uncertainty. We consider the m_{ES} distribution from the data and the combinatorial $B\overline{B}$ continuum and other background components (cascade and hadronic B decays) modeled with distributions taken from the Monte Carlo simulation. We fit the background normalization on data in the m_{ES} sideband region, defined by $m_{ES} < 5.265 \text{ GeV}/c^2$. The normalization for the continuum background is fixed to the value obtained from off-peak data. The total background contribution is then subtracted by the total number of events in the m_{ES} distribution to extract the $\overline{B} \rightarrow X\ell^-\bar{\nu}_\ell$ signal yield. The uncertainty in the determination of the $\overline{B} \rightarrow D^{(*)}(\pi)\ell^-\bar{\nu}_\ell$ yield is estimated by

changing the PDFs used to model the different contributions in the m_{miss}^2 distribution, e.g. by replacing the continuum PDFs with the corresponding one obtained from off-peak data.

6 Results

We measure the following branching fractions:

$$\begin{aligned}
\mathcal{B}(B^- \rightarrow D^0 \ell^- \bar{\nu}_\ell) &= (2.33 \pm 0.09_{stat.} \pm 0.09_{syst.})\% \\
\mathcal{B}(B^- \rightarrow D^{*0} \ell^- \bar{\nu}_\ell) &= (5.83 \pm 0.15_{stat.} \pm 0.30_{syst.})\% \\
\mathcal{B}(\bar{B}^0 \rightarrow D^+ \ell^- \bar{\nu}_\ell) &= (2.21 \pm 0.11_{stat.} \pm 0.12_{syst.})\% \\
\mathcal{B}(\bar{B}^0 \rightarrow D^{*+} \ell^- \bar{\nu}_\ell) &= (5.49 \pm 0.16_{stat.} \pm 0.25_{syst.})\% \\
\mathcal{B}(B^- \rightarrow D^+ \pi^- \ell^- \bar{\nu}_\ell) &= (0.42 \pm 0.06_{stat.} \pm 0.03_{syst.})\% \\
\mathcal{B}(B^- \rightarrow D^{*+} \pi^- \ell^- \bar{\nu}_\ell) &= (0.59 \pm 0.05_{stat.} \pm 0.04_{syst.})\% \\
\mathcal{B}(\bar{B}^0 \rightarrow D^0 \pi^+ \ell^- \bar{\nu}_\ell) &= (0.43 \pm 0.08_{stat.} \pm 0.03_{syst.})\% \\
\mathcal{B}(\bar{B}^0 \rightarrow D^{*0} \pi^+ \ell^- \bar{\nu}_\ell) &= (0.48 \pm 0.08_{stat.} \pm 0.04_{syst.})\%.
\end{aligned} \tag{2}$$

We compute the total branching fractions of the $\bar{B} \rightarrow D^{(*)} \pi \ell^- \bar{\nu}_\ell$ decays assuming isospin symmetry, $\mathcal{B}(\bar{B} \rightarrow D^{(*)} \pi^0 \ell^- \bar{\nu}_\ell) = \frac{1}{2} \mathcal{B}(\bar{B} \rightarrow D^{(*)} \pi^\pm \ell^- \bar{\nu}_\ell)$, to estimate the branching fractions of $D^{(*)} \pi^0$ final states. We obtain:

$$\begin{aligned}
\mathcal{B}(B^- \rightarrow D^{(*)} \pi \ell^- \bar{\nu}_\ell) &= (1.52 \pm 0.12_{stat.} \pm 0.10_{syst.})\% \\
\mathcal{B}(\bar{B}^0 \rightarrow D^{(*)} \pi \ell^- \bar{\nu}_\ell) &= (1.37 \pm 0.17_{stat.} \pm 0.10_{syst.})\%,
\end{aligned} \tag{3}$$

where we assume the systematic uncertainties on the $\bar{B} \rightarrow D \pi \ell^- \bar{\nu}_\ell$ and $\bar{B} \rightarrow D^* \pi \ell^- \bar{\nu}_\ell$ modes to be completely correlated. The accuracy of the branching fraction measurement for the $\bar{B} \rightarrow D^{(*)} \ell^- \bar{\nu}_\ell$ decays is comparable to that of the current world average [2]. The result for the $\bar{B} \rightarrow D^{(*)} \pi \ell^- \bar{\nu}_\ell$ branching fraction is comparable with the BELLE result [12].

In conclusion, preliminary results of the branching fractions of exclusive B semileptonic decays have been obtained for the $\bar{B} \rightarrow D^{(*)}(\pi) \ell^- \bar{\nu}_\ell$ modes.

7 Acknowledgments

We are grateful for the extraordinary contributions of our PEP-II colleagues in achieving the excellent luminosity and machine conditions that have made this work possible. The success of this project also relies critically on the expertise and dedication of the computing organizations that support *BABAR*. The collaborating institutions wish to thank SLAC for its support and the kind hospitality extended to them. This work is supported by the US Department of Energy and National Science Foundation, the Natural Sciences and Engineering Research Council (Canada), Institute of High Energy Physics (China), the Commissariat à l’Energie Atomique and Institut National de Physique Nucléaire et de Physique des Particules (France), the Bundesministerium für

Bildung und Forschung and Deutsche Forschungsgemeinschaft (Germany), the Istituto Nazionale di Fisica Nucleare (Italy), the Foundation for Fundamental Research on Matter (The Netherlands), the Research Council of Norway, the Ministry of Science and Technology of the Russian Federation, and the Particle Physics and Astronomy Research Council (United Kingdom). Individuals have received support from the Marie-Curie IEF program (European Union) and the A. P. Sloan Foundation.

References

- [1] M. Kobayashi and T. Maskawa, Prog. Theor. Phys. **49**, 652 (1973).
- [2] W. M. Yao *et al.* (Particle Data Group), J. Phys. G **33**, 1 (2006).
- [3] Heavy Flavor Averaging Group, <http://www.slac.stanford.edu/xorg/hfag/semi/pdg07/home.shtml>
- [4] N. E. Adam *et al.* (CLEO Collaboration), Phys. Rev. D **67**, 032001 (2003) .
- [5] B. Aubert *et al.* (BABAR Collaboration), arXiv:0707.2655.
- [6] D. Buskulic *et al.* (ALEPH Collaboration), Z. Phys. C **73**, 601 (1997).
- [7] P. Abreu *et al.* (DELPHI Collaboration), Phys. Lett. B **475**, 407 (2000).
- [8] D. Bloch *et al.* (DELPHI Collaboration), DELPHI 2000-106 CONF 405.
- [9] G. Abbiendi *et al.* (OPAL Collaboration), Eur. Phys. J. C **30**, 467 (2003).
- [10] A. Anastassov *et al.* (CLEO Collaboration), Phys. Rev. Lett. **80**, 4127 (1998).
- [11] V. M. Abazov *et al.* (D0 Collaboration), Phys. Rev. Lett. **95**, 171803 (2005).
- [12] D. Liventsev *et al.* (Belle Collaboration), Phys. Rev. D **72**, 051109 (2005).
- [13] B. Aubert *et al.* (BABAR Collaboration), hep-ex/0703027, accepted by PRD.
- [14] B. Aubert *et al.* (BABAR Collaboration), Nucl. Inst. Meth. A **479**, 1 (2002).
- [15] S. Agostinelli *et al.*, Nucl. Inst. Meth. A **506**, 250 (2003).
- [16] B. Aubert *et al.* (BABAR Collaboration), arXiv:0705.4008 [hep-ex], submitted to PRD.
- [17] D. Scora and N. Isgur, Phys. Rev. D **52**, 2783 (1995). See also N. Isgur *et al.*, Phys. Rev. D **39**, 799 (1989).
- [18] J. L. Goity and W. Roberts, Phys. Rev. D **51**, 3459 (1995).
- [19] B. Aubert *et al.* (BABAR Collaboration), Phys. Rev. D **69**, 111104 (2004).
- [20] H. Albrecht *et al.* (ARGUS Collaboration), “Exclusive semileptonic decays of B mesons to D mesons”, DESY-92-029 (1992).
- [21] R. J. Barlow and C. Beeston, Comput. Phys. Commun. **77**, 219 (1993).
- [22] B. Aubert *et al.* (BABAR Collaboration), Phys. Rev. D **74**, 091105 (2006).

- [23] H. Albrecht *et al.* (ARGUS Collaboration), *Z. Phys.* **C48**, 543 (1990).
- [24] M. J. Oreglia, SLAC-236 (1980); J. E. Gaiser, SLAC-255 (1982); T. Skwarnicki, DESY F31-86-02 (1986).

Table 3: Systematic uncertainties (relative errors in %) in the measurement of $\Gamma(\overline{B} \rightarrow D^{(*)} \ell^- \bar{\nu}_\ell) / \Gamma(\overline{B} \rightarrow X \ell^- \bar{\nu}_\ell)$.

	Systematic uncertainty on $\Gamma(\overline{B} \rightarrow D^{(*)} \ell^- \bar{\nu}_\ell) / \Gamma(\overline{B} \rightarrow X \ell^- \bar{\nu}_\ell)$			
	$B^- \rightarrow D^0 \ell^- \bar{\nu}_\ell$	$B^- \rightarrow D^{*0} \ell^- \bar{\nu}_\ell$	$\overline{B}^0 \rightarrow D^+ \ell^- \bar{\nu}_\ell$	$\overline{B}^0 \rightarrow D^{*+} \ell^- \bar{\nu}_\ell$
Tracking efficiency	1.4	1.2	1.4	1.5
Neutral reconstruction	0.7	1.9	0.5	1.1
lepton ID	0.5	0.4	0.5	0.6
Soft particle efficiency	-	1.3	-	1.2
Monte Carlo corrections				
Conversion and Dalitz decay background	0.04	0.07	0.06	0.05
Cascade $\overline{B} \rightarrow X \rightarrow \ell^-$ decay background	0.6	0.6	1.0	1.0
$\overline{B}^0 - B^-$ cross-feed	0.2	0.3	0.2	0.3
Form factors	0.4	0.8	0.4	0.8
$D^{(*)}$ branching fractions	2.3	3.5	4.1	2.7
$\overline{B} \rightarrow X \ell^- \bar{\nu}_\ell$ branching fraction	1.9	1.9	1.9	1.9
B_{tag} selection	0.9	1.7	1.8	1.3
Fit technique				
$\overline{B} \rightarrow X \ell^- \bar{\nu}_\ell$ yield	0.5	0.5	0.9	0.9
$\overline{B} \rightarrow D^{(*)} \ell^- \bar{\nu}_\ell$ yield	0.6	0.4	1.2	0.4
Total systematic error	3.7	5.2	5.4	4.5

Table 4: Systematic uncertainties (relative errors in %) in the measurement of $\Gamma(\overline{B} \rightarrow D^{(*)}\pi\ell^-\bar{\nu}_\ell)/\Gamma(\overline{B} \rightarrow X\ell^-\bar{\nu}_\ell)$.

	Systematic uncertainty on $\Gamma(\overline{B} \rightarrow D^{(*)}\pi\ell^-\bar{\nu}_\ell)/\Gamma(\overline{B} \rightarrow X\ell^-\bar{\nu}_\ell)$			
	$B^- \rightarrow D^+\pi^-\ell^-\bar{\nu}_\ell$	$B^- \rightarrow D^{*+}\pi^-\ell^-\bar{\nu}_\ell$	$\overline{B}^0 \rightarrow D^0\pi^+\ell^-\bar{\nu}_\ell$	$\overline{B}^0 \rightarrow D^{*0}\pi^+\ell^-\bar{\nu}_\ell$
Tracking efficiency	1.8	2.7	1.5	1.7
Neutral reconstruction	1.7	1.8	1.1	1.8
lepton ID	2.3	3.0	2.6	1.8
Soft particle efficiency	-	1.2	-	1.3
Monte Carlo corrections				
Conversion and Dalitz decay background	0.15	0.4	0.05	0.2
Cascade $\overline{B} \rightarrow X \rightarrow \ell^-$ decay background	0.6	0.6	1.0	1.0
$\overline{B}^0 - B^-$ cross-feed	0.2	0.3	0.2	0.3
Form factors	0.4	0.8	0.4	0.8
$D^{(*)}$ branching fractions	4.2	2.9	2.5	4.4
$\overline{B} \rightarrow X\ell^-\bar{\nu}_\ell$ branching fraction	1.9	1.9	1.9	1.9
B_{tag} selection	5.0	4.3	4.0	5.6
Fit technique				
$\overline{B} \rightarrow X\ell^-\bar{\nu}_\ell$ yield	0.5	0.5	0.9	0.9
$\overline{B} \rightarrow D^{(*)}\pi\ell^-\bar{\nu}_\ell$ yield	1.2	0.9	1.8	1.5
Total systematic error	7.7	7.3	6.4	8.4